International Journal of GEOMATE, April, 2020, Vol.18, Issue 68, pp. 180 - 186
ISSN: 2186-2982 (P), 2186-2990 (O), Japan, DOI: https://doi.org/10.21660/2020.68.9340
Special Issue on Science, Engineering and Environment

STUDY ON THE ESTIMATION OF MICROWAVE LAND SURFACE EMISSIVITY OVER EAST ASIA

*Nozomu Hirose[1], Kenji Taniguchi[2] and Ichirow Kaihotsu[3]

[1]National Institute of Technology, Matsue College, Japan; [2] Faculty of Geosciences and Civil Engineering, Kanazawa University, Japan; [3] Hiroshima University, Japan

*Corresponding Author, Received: 30 July 2019, Revised: 30 Nov. 2019, Accepted: 03 Feb. 2020

ABSTRACT: Estimation of the land surface emissivity is crucial to evaluate the boundary conditions of atmospheric modeling data assimilation. Brightness temperatures observed by satellite passive microwave radiometer give information on emission forma raindrops and scattering by frozen particles. By applying radiative transfer model of the atmosphere, we can estimate the atmospheric hydrological process (i. e., rainfall, snowfall, water vapor, cloud water, etc.). However it is difficult to estimate microwave land surface emissivity at higher frequencies over land. Because land use, land cover and surface wetness over land are various and heterogeneous by comparing with over ocean. Therefore, we aim to estimate the microwave land surface emissivity over East Asia by using observed data and numerical models.

Firstly, we investigate the characteristics of land surface emissivity derived from SSM/I, AMSR-E and AMSR2 over Asia and the relationship between land surface emissivity and land hydrological variables based on satellite data sets and numerical models. Secondary, we estimate the land surface emissivity by applying the Community Microwave Emission Model (CMEM) and Community Radiative Transfer Model (CRTM).

Simulation results shows the estimated LSE is overestimated and its variability is large by comparing the observed data.

Keywords: Microwave land surface emissivity, Radiative transfer model, Passive microwave remote sensing, Mongolia, Field observation datasets

1. INTRODUCTION

Microwave land surface emissivity at higher frequencies is crucial for cloud data assimilation for heavy rainfall. Cloud data assimilation has great potential to improve the prediction of heavy rainfall area because it can directly obtain information on locations of rain systems. Clouds can be observed globally by satellite-based microwave remote sensing. Therefore, satellite-based microwave remote sensing has Retrievals of land surface emissivity (LES) are challenging due to the high variability of emissivity and its sensitivity to land surface hydrological parameters [1], [2], [3]. Passive microwave remote sensing such as AMSR-E and AMSR2 has the advantages of considerably high revisit time and having multiple channels that are sensitive to different atmospheric variables and surface properties [4], [5], [6].

The objectives of our study are to investigate the temporal and spatial variability of LSE over East Asia, to reveal the relationship between LES at low frequency (6.9GHz and 10.7GHz) and high frequency (36.5GHz and 89.0GHz) by exploring the AMSR-E Monthly Global Microwave LSE dataset obtained from National Snow and Ice Data Center (NSIDC) and to estimate the LES at Mongolia observation sites from 2002 to 2008 by applying the Community Microwave Emission Model (CMEM) and Community Radiative Transfer Model (CRTM).

CMEM is developed by ECMWF for low frequency passive microwave brightness temperatures from 1 GHz to 20 GHz of the surface.

To estimate LES at higher frequencies by applying CMEM, we should clarify the relationship of LES between low and high frequency using NSIDC LES data set. On the other hand, CRTM with the land microwave emissivity component is used in a wide frequency range from 1 GHz to 100 GHz. Microwave LES at higher frequency is directly estimated by applying CRTM.

2. RESULTS

Microwave land surface emissivity strongly depends on the land surface condition (i. e., land use, land cover, vegetation type, surface wetness, surface roughness, etc.). Therefore, we investigate the relationship between land surface emissivity and land use by using satellite observation date.

All of the seven channels with vertical and horizontal polarizations of AMSR-E/Aqua Global Monthly LSE at 0.25° latitude/longitude for the study period from July 2002 to June 2008 were obtained from data providing service at NSIDC. Our target areas are Mongolian Plateau and Japan.

2.1 Characteristics of Microwave Land Surface Emissivity over East Asia

2.1.1 Mongolian Plateau

Firstly, Mongolian Plateau area is shown in Fig. 1a. These figures also show the classification of land cover by using the dataset of USGS (Unite States Geological Survey) Global Land Cover Characterization (GLCC) Version 2.0. Table 1 shows the category of GLCC value.

Fig. 1b shows the relative frequency of land cover in the histogram. Glassland, shrub land and Barren or Sparesly vegetated are mainly covered with our target area. The characteristics of land cover in our area is less vegetated condition.

Table 1 Category of GLCC version 2.0

Value	Class Name
1	Urban and Built-Up Land
2	Dryland Cropland and Pasture
3	Irrigated Cropland and Pasture
4	Mixed Dryland/Irrigated Cropland and Pasture
5	Cropland/Grassland Mosaic
6	Cropland/Woodland Mosaic
7	Grassland
8	Shrubland
9	Mixed Shrubland/Grassland
10	Savanna
11	Deciduous Broadleaf Forest
12	Deciduous Needleleaf Forest
13	Evergreen Broadleaf Forest
14	Evergreen Needleleaf Forest
15	Mixed Forest
16	Water Bodies
17	Herbaceous Wetland
18	Wooded Wetland
19	Barren or Sparsely Vegetated
20	Herbaceous Tundra
21	Wooded Tundra
22	Mixed Tundra
23	Bare Ground Tundra
24	Snow or Ice

2.1.2 Japan

Secondary, Japan area is shown in Fig. 2a. These figures also show the classification of land cover by using the dataset of USGS (Unite States Geological Survey) Global Land Cover Characterization Version 2.0. Fig.2 shows the relative frequency of land cover in the histogram. Forest is mainly covered with our target area. The characteristics of land cover in our area is more vegetated condition.

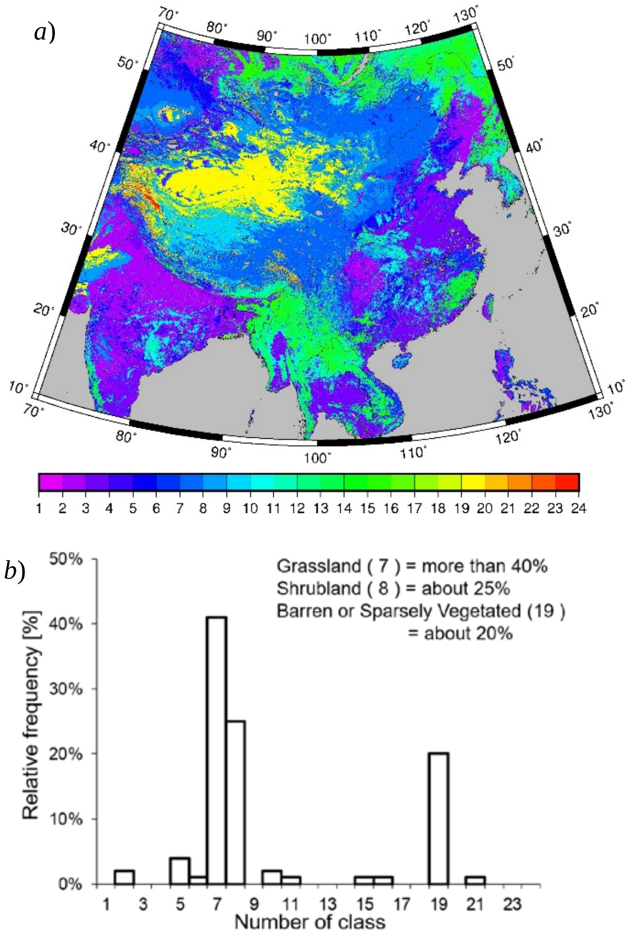

Fig. 1 *a*) Land cover classes and *b*) the relative frequency of land cover over Mongolian Plateau.

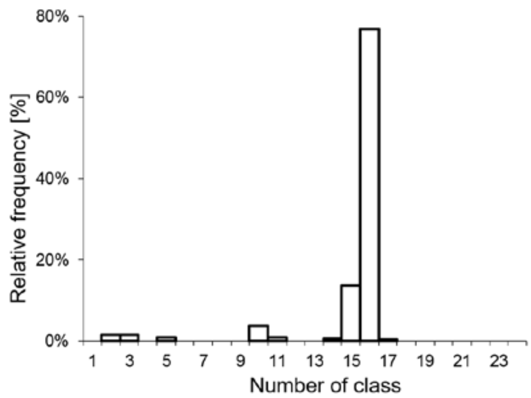

Fig. 2 Relative frequency of land cover classes over Japan.

As compared with Mongolian Plateau, Japan area is covered with forest more than 90% as show in Fig. 4.

2.2 Relationship between LES at Low Frequency and High Frequency

2.2.1 Mongolian Plateau

Fig. 3a presents the comparison between land surface emissivity at low frequencies (6.9GHz and 10.7GHz) and other high frequencies in July 2002 at grassland area. It represents the relationship between land surface emissivity and land hydrological variables (land type, land use, vegetation and soil moisture) in summer. The LSE at 6.9GHz with horizontal polarization is related with at higher frequencies.

However, variation is large in the relationship between LSE at 6.9GHz and at 89.0GHz with horizontal polarization.

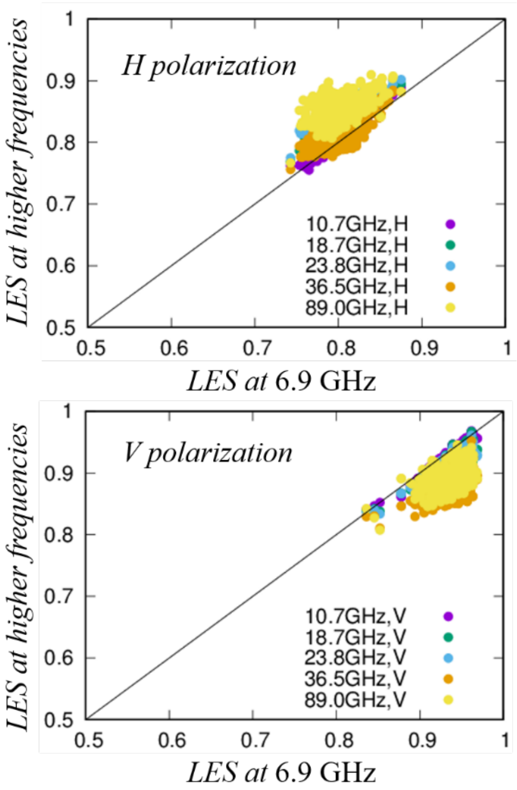

Fig. 3a Relationship between LES at 6.9 GHz and LES at higher frequency with horizontal (*H*) and vertical (*V*) polarization over grassland area in July 2002 shown in Fig. 1a.

Fig. 3b shows the comparison between LSE at low and high frequencies at bare soil area. By comparing Fig. 3a, we found that liner relationship between LES at 6.9 GHz and LES at higher frequency with both polarization is clear. Therefore, these figures imply that microwave LSE at high frequency, 89.0GHz can be estimated by using microwave low-frequency LES in summer.

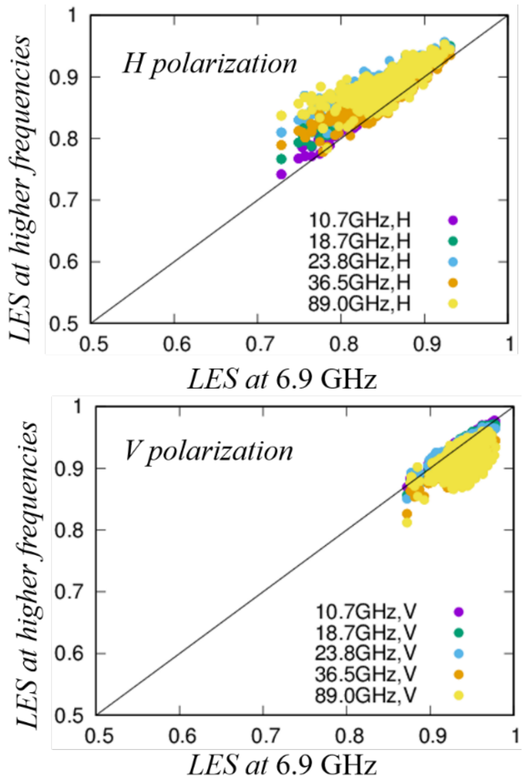

Fig. 3b Relationship between LES at 6.9 GHz and LES at higher frequency with horizontal (*H*) and vertical (*V*) polarization over bare soil area in July 2002 shown in Fig. 1a.

2.2.2 Seasonal change of LES relationship in Mongolian Plateau

Fig.4 shows the seasonal change of the relationship between low-frequencies and high frequency LES over barren or sparsely vegetated area. It is found that correlation coefficient in summer (from July to September) is higher compared with one in winter. The correlation coefficient is more than 0.8 and the slope of the linear regression line in Fig.4a is from 0.52 to 0.64 from July to September. This figure shows that high frequency LES can be estimated by using low frequency LES.

On the other hands, the correlation coefficient is low from October to February. This means surface ground temperature decreases less than 0 degree Celsius from fall to winter and surface ground is frozen in winter.

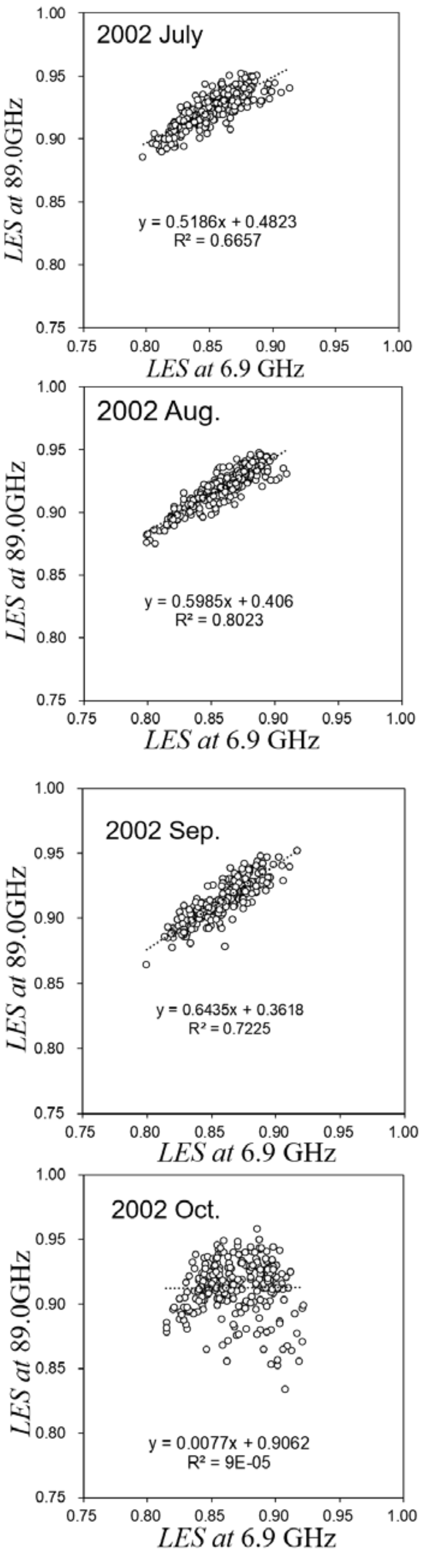

Fig. 4a Seasonal change of relationship between LES at 6.9GHz and LES at 89.0GHz with horizontal polarization from July 2002 to October 2002 at bare soil area shown in Fig. 1a.

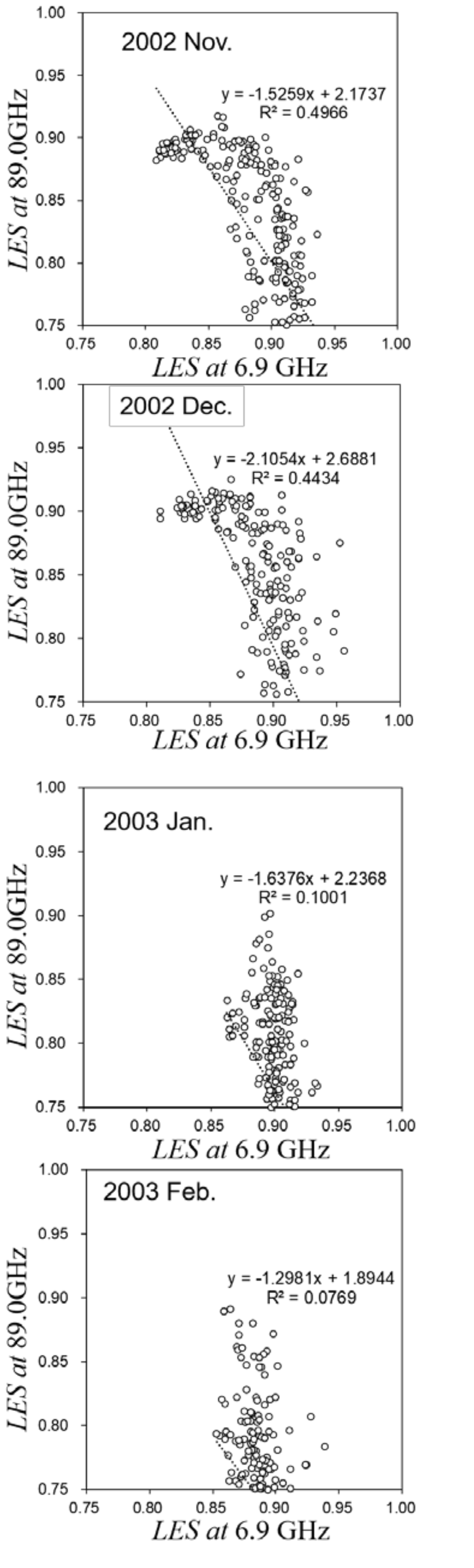

Fig. 4b Seasonal change of relationship between LES at 6.9GHz and LES at 89.0GHz with horizontal polarization from November 2002 to February 2003 at bare soil area shown in Fig. 1a.

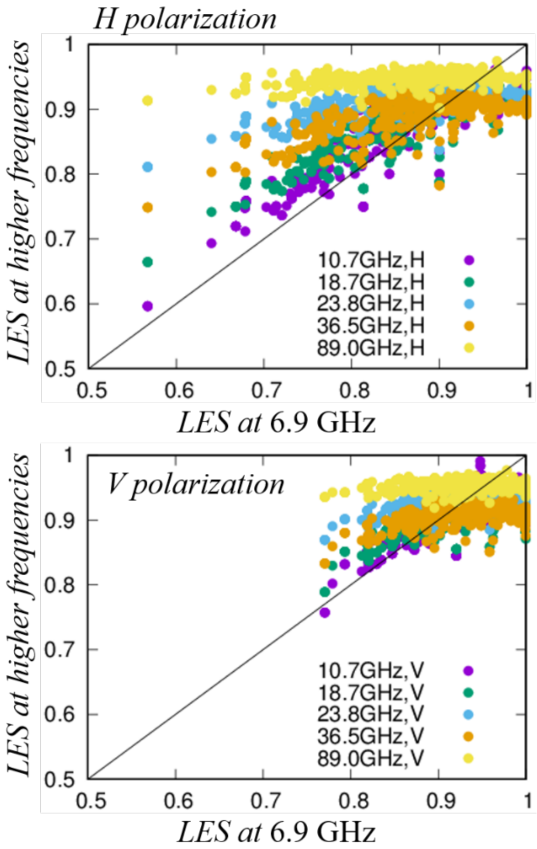

Fig. 5a Relationship between LES at 6.9 GHz and LES at higher frequency with horizontal (H) and vertical (V) polarization over Japan.in July 2002.

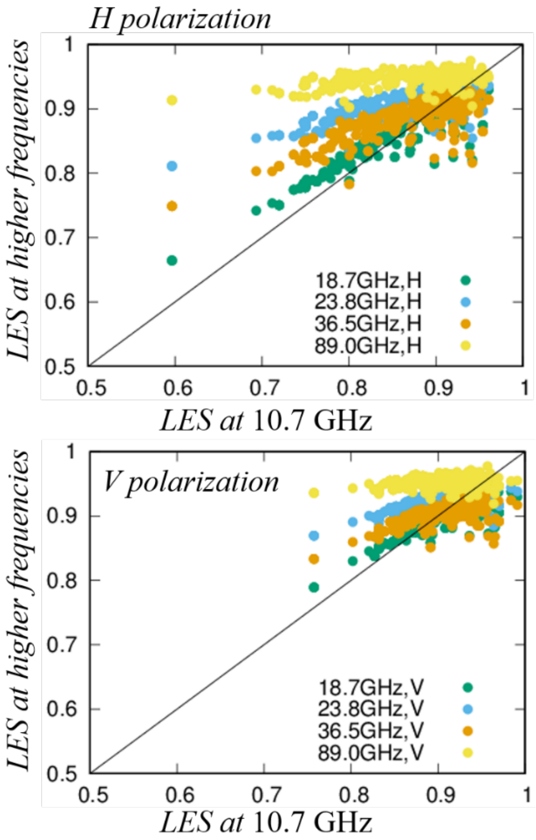

Fig. 5b Relationship between LES at 10.7 GHz and LES at higher frequency with horizontal (H) and vertical (V) polarization over Japan.in July 2002.

2.2.3 Japan

Fig. 5 presents the comparison between land surface emissivity at low frequencies (6.9GHz and 10.7GHz) and other high frequencies in July 2002 in Japan as shown in Fig.2a.

However, variation is large in the relationship between LSE at 6.9GHz and at 89.0GHz with horizontal and vertical polarization in July 2002. Because Japan area has diverse land cover and is mainly covered with mixed forest, LSE at 6.9GHz is not correct.

This figure shows that high frequency LES cannot be estimated by using low frequency LES.

3. ESTIMATION OF LAND SURFACE EMISSIVITY

The Community Microwave Emission Model, CMEM comprises the physics and parameterizations used in the Land Surface Microwave Emission Model (LSMEM) [7] and the L-Band Microwave Emission of the Biosphere (L-MEB) [8], [9].

3.1 Community Microwave Emission Model (CMEM)

CMEM was developed by the ECMWF for numerical weather prediction applications and is used to simulate passive microwave brightness temperatures of the surface at low frequencies (from 1 GHz to 20 GHz) [10], [11], [12]. For polarization (p), the brightness temperatures over snow-free areas at the top of the atmosphere (TOA) TBtoa,p, which result from the contributions of three dielectric layers (soil, vegetation, and atmosphere), can be expressed as follows:

$$T_{Btoa,p} = T_{Bau,p} + e^{-\tau_{atm,p}} \cdot T_{Btov,p} \quad (1)$$

$$T_{Btov,p} = T_{Bsoil,p} \cdot e^{-\tau_{veg,p}} + T_{Bveg,p}(1 + r_{r,p} \cdot e^{-\tau_{veg,p}}) + T_{Bad,p} \cdot r_{r,p} \cdot e^{-2\tau_{veg,p}} \quad (2)$$

where TBtov,p is the top-of-vegetation brightness temperature when the vegetation is represented as a single-scattering layer above a rough surface; τatm,p is the atmospheric optical depth; TBau,p and TBad,p are the upward and downward atmospheric emissions, respectively; and TBsoil,p and TBveg,p are the soil and vegetation layer contributions, respectively. Here, rr,p is the soil reflectivity of a rough surface (one minus the emissivity er,p), and τveg,p is the vegetation optical depth along the viewing path.

3.2 Simulation Results

We address long-term land hydrological dataset measured at Mongolia observation sites. By applying to CMEM, microwave land surface emissivity at 6.9GHz with horizontal and vertical polarization are estimated at Mongolia site.

Fig. 6a and 6b present the comparison between simulation results at Mongolia site by using CMEM and AMSR-E Monthly Global LSE. Fig. 4a shows the simulated microwave LSE at 6.9GHz with horizontal polarization is overestimated and its temporal variability is very large.

On the other hand, Fig. 5b shows the simulation result with vertical polarization is good agreement with AMSR-E Monthly LSE at Mongolia observation site.

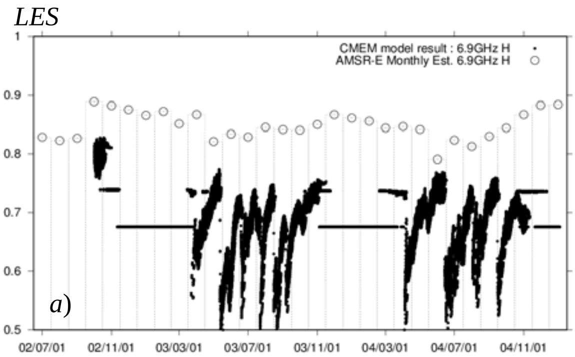

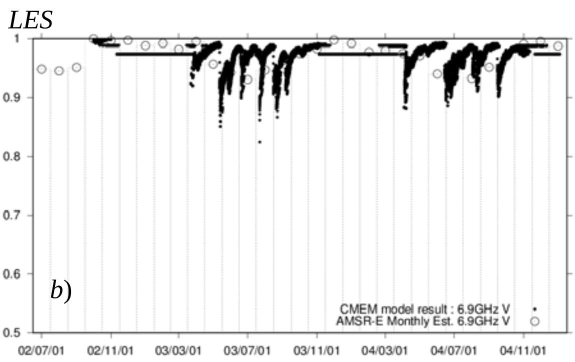

Fig 6. Comparison between the observed microwave LES (open circle) and simulation results (solid circle) with a) Horizontal polarization and b) Vertical polarization.

4. CONCLUTION

In this study, we investigate the temporal and spatial variability of LSE over Asia and the relationship between LES at low frequency (6.9GHz and 10.7GHz) and high frequency (36.5GHz and 89.0GHz) and try to estimate microwave land surface emissivity from July 2002 to January 2005 at Mongolia observation sites.

Firstly, Microwave LES at high frequencies is related to LES at low frequencies in summer. It implies effect of land surface hydrological variables to LES. Therefore, we try to identify the effect of snow, vegetation type and soil moisture by using Land use and MODIS dataset. Secondly, Microwave LES at 6.9GHz with horizontal and vertical polarization is simulated at Mongolia observation sites. Simulation results shows the estimated LSE is overestimated and its variability is large by comparing the observed data.

We should reveal the effect of snow and vegetation type to the relationship between LES at low and high frequencies and calibrate CMEM model parameters to represent the temporal and spatial variability of LSE obtained from AMSR-E and AMSR2.

5. ACKNOWLEDGMENTS

The data sources used in the study are graciously acknowledged. This work was supported by JAXA PMM RA8 and JSPS KAKENHI Grant Number JP26289162.

6. REFERENCES

[1] Hirose, N., K. Taniguchi, and I. Kaihotsu, Estimation of land surface emissivity for atmospheric modelling data assimilation. Abstracts of the 61th autumn conference of the remote sensing society of japan, B15, 2016, pp.10.

[2] Hirose, N., K. Taniguchi, and I. Kaihotsu, Relationship between land surface emissivity and land hydrological variables. Proceeding of International Symposium on Remote Sensing 2017, D-37, 2017, pp.507-508.

[3] N. Hirose, K. Taniguchi, and I. Kaihotsu, Estimation of microwave land surface emissivity over East Asia, 39th Asian Conference on Remote Sensing 2018 Proceeding, 2018, pp.1567-1569.

[4] Tian, Y., C. D. Peters-Lidard, K. W. Harrison, Y. You, S. Ringerud, S. Kumar, and F. J. Turk, An examination of methods for estimating land surface microwave emissivity, J. Geophys. Res. Atmos., 120, 2015, pp.11,114–11,128, doi:

10.1002/2015JD023582.
[5] Prakash, S., H. Norouzi, M. Azarderakhsh, R. Blake, and K. Tesfagiorgis, Global land surface emissivity estimation from AMSR2 observations, IEEE Geoscience and Remote Sensing Letters, 13(9), 2016, pp.1270-1274.
[6] de Rosnay, P., M. Drusch and J. Muñoz Sabater, Milestone 1 Tech Note - Part 1: SMOS Global Surface Emission Model, 2009a, p.1-15.
[7] de Rosnay P., M. Drusch, A. Boone, G. Balsamo, B. Decharme, P. Harris, Y. Kerr, T. Pellarin, J. Polcher and J.-P. Wigneron, The AMMA Land Surface Model Intercomparison Experiment coupled to the Community Microwave Emission Model: ALMIP-MEM. J. Geophys. Res., Vol 114, 2009b, p.18, doi:10.1029/2008JD010724.
[8] Drusch, M. and Jacson, T., Vegetative and atmospheric corrections for soil moisture retrieval from passive microwave remote sensing data: Results from the Southern Great Plains Hydrology Experiment 1997. J. Hydrometeor., 2, 2001, pp.181-192.
[9] Wigneron J.P., Kerr Y., Waldteufel P., Saleh K., Escorihuela M.J., Richaume P., Ferrazzoli P., De Rosnay P., Gurney R., and Calvet J.C., L-band Microwave Emission of the Biosphere (L-MEB) model: Description and calibration against experimental data sets over crop fields. Remote Sens. Environ., 107, 2007, pp.639-655.
[10] Holmes, T., M. Drusch, J.-P. Wigneron, and R. de Jeu, A global simulation of microwave emission: Error structures based on output from ECMWF's operational Integrated Forecast System, IEEE Trans. Geosci. Remote Sens., 46, 2008, pp.846–856.
[11] Drusch, M., T. Holmes, P. de Rosnay, and G. Balsamo, Comparing ERA-40 based L-band brightness temperatures with Skylab observations: A calibration/validation study using the Community Microwave Emission Model, J. Hydrometeor., 10, 2009, pp.213–226.
[12] Jia, B., and Z. Xie, Evaluation of the community microwave emission model coupled with the community land model over East Asia. Atmospheric and Oceanic Science Letters, 4, 2011, pp.209–215.